Journal of Thermal Analysis and Calorimetry, Vol. 92 (2008) 3, 783–789

CALORIMETRIC STUDY OF DISSOLUTION KINETICS OF PHOSPHORITE IN DILUTED ACETIC ACID

T. C. Vaimakis[1*], *E. D. Economou*[1] *and C. C. Trapalis*[2]

[1]University of Ioannina, Department of Chemistry, P.O. Box 1186, 45110 Ioannina, Greece
[2]National Center for Scientific Research 'Demokritos', Institute of Materials Science, 153 10 Athens, Greece

In this report, we present a thermodynamic and kinetic study of the selective dissolution of calcite from low-grade phosphate ores (Epirus area, Greece) by dilute acetic acid at isothermal conditions. A twin calorimeter with two identical membrane vessels, for the acid dissolution process, and for the reference was used. The curves of rate *vs*. time of the phosphorite dissolution for various temperatures show that the maximum ($\dot{q}_{max}$) was increased, whereas the time (t_{peak}) to achieve the corresponding $\dot{q}_{max}$ values was decreased, as the experimental temperature was increased. The dissolution enthalpy was increased from 13.1 to 16.7 kJ mol^{-1}, as the experimental temperature was increased from 10.0 to 28.0°C. The chemical analysis of the supernatant solutions shows that the main process was the calcite dissolution. The reaction model with general form, $\ln(1/(1-X))=kt^m$, was found to fitted the experimental data regardless of the experimental temperature. These results were assigned in the presence of two different kinds of particles in the phosphorite. The activation energy of the dissolution process was found 69.7 kJ mol^{-1}. The SEM micrographs of acid dissolution samples showed two different textures after acid dissolution.

Keywords: *calorimetric, kinetic mechanism, phosphorite dissolution*

Introduction

The phosphorite deposits in the Epirus area (Greece) are sedimentary low-grade phosphate ores composed of minerals of francolite (carbonate fluorapatite with empirical formula $Ca_{9.51}Na_{0.35}MgO_{0.14}(PO_4)_{4.74}(CO_3)_{1.26}F_{2.50}$) and calcite. As a result of the intimate mixture of these two minerals and hardness of ore, there is no feasible physical or physicochemical method of producing feed suitable for acidic phosphorite digestion or leaching processes. A number of contributions on the enrichment of the low-grade calcareous phosphate ores by selective dissolution of calcite species using weak organic acids have been presented [1–8]. The kinetics of carbonate dissolution is very sensitive to the surface structure, composition, and physical properties of crystals, and it is strongly dependent on the pH value of the reaction solution.

The treatment of calcite dissolution kinetics was based on Plummer, Wigley, and Parkhust (PWP) model (Eq. (1)), derived by probable chemical reactions occurring at the crystal surface [9, 10].

$$R = k_1(H^+) + k_2\alpha(H_2CO_3^*) + k_3\alpha(H_2O) - k_4\alpha(Ca^{2+})\alpha(HCO_3^-) \quad (1)$$

where R means reaction rate, k_1 to k_4 are rate constants, α means the activities of reactants of the dissolving mineral, and $H_2CO_3^*$ denotes the sum of H_2CO_3 and dissolved CO_2.

As it has been thoroughly described by Compton *et al.* [11, 12] calcite dissolution could be discussed in terms of two main regimes: (a) at a low pH-regime (<4), where the process of dissolution of calcite is controlled by the surface heterogeneous first-order reaction (2), and (b) at alkaline pH range, where the dissolution process is more complicated, and the reaction (3) should be considered as the important one.

$$CaCO_3 + H^+ \rightarrow Ca^{2+} + HCO_3^- \quad (2)$$

$$CaCO_3 \rightarrow Ca^{2+}_{(aq)} + CO_3^{2-} \quad (3)$$

Sjöberg and Rickard [13] studied the calcite dissolution by applying rotation disc electrode technique. Generally, calcite dissolution could be discussed in terms of three regimes. At low-pH regime (<4.5) H^+ ions penetrate the diffusion boundary layer, and reach the calcite surface; accordingly, the rate of calcite dissolution depends on the square root of the surface concentration of $[H^+]$. At pH-values >5.5, the dissolution rate of calcite is independent of $[H^+]$. In the latter case the mechanism involves transport of the produced calcium and carbonate ions out to diffusion boundary layer interface, where rapid protonation reactions occur. For pH values between 4.0 and

* Author for correspondence: tvaimak@cc.uoi.gr

1388–6150/$20.00

Akadémiai Kiadó, Budapest, Hungary
Springer, Dordrecht, The Netherlands

5.5 there is a transition regime. Al-Khaldi *et al.* [14] studied the dissolution of the calcite with citric acid by rotating disk apparatus. They found that the reaction mechanism of citric acid and calcite is mass-transfer and the reaction rate limited by the precipitation of calcium citrate on the surface.

Economou *et al.* [15] found that the dissolution of $CaCO_3$ by dilute phosphoric acid is based on the adsorption of phosphoric acid on the $CaCO_3$ surface. Recently, two review papers were published on the dissolution kinetics of sedimentary carbonate minerals [16, 17].

In a previous paper [3] we reported the most effective conditions of the selective dissolution of calcite from low-grade phosphate ores originated from Epirus–Greece area, using dilute acetic acid. In more recent studies [5, 6] we reported the detailed mechanism of the process in the pH range from 2.37 to 6.40 by recording the pH changes of the reaction medium *vs*. time. The selective dissolution of calcite from low-grade phosphate ores by acids is based on the relatively higher rate of acid dissolution of $CaCO_3$, than that of calcium phosphate. The Greek phosphate ores have a complicated structure, consisted from laminas of pure calcite, phoshopelloid particles and calcite in the spaces between phospho-pelloids particles. During the dissolution process the calcite species were mainly dissolved, whereas almost all of the francolite remained in the solid phase. The calcite dissolution process took place in two steps. It starts along with dissolution of the released calcite particles and/or species on particles, and continues by the dissolution of calcite in the interspaces between phospopelloid particles. Hence, in the first approach [3, 4] we approximated the enrichment procedure of these phosphate ores for both described steps by the reaction model with general form:

$$\ln\frac{1}{1-X}=kt^{m} \text{ or } \ln[-\ln(1-X)]=\ln k+m\ln t \qquad (4)$$

where X is the conversion fraction, t is the time, k is a rate constant, and value parameter m depends on the reaction mechanism. The two above mentioned dissolution steps can be represented by the followed empirical equations:

1st step: $-\ln(1-X)=0.0736t^{0.447}$ [3] (5)

or $-\ln(1-X)=0.0766t^{0.442}$ [4] (5a)

2nd step: $-\ln(1-X)=0.566t^{0.163}$ [3] (6)

In order to understand the exact significance of m variations, is necessary to know the changes in the degree of interaction of the acid solution and the influence of the respective acid anion [3, 18]. Equation (4) is widely used as a probe for preliminary identification of the rate law. Magnitudes of m have been empirically developed according to the circumstances. For diffusion-limited equations the values of m usually vary between 0.53 and 0.58 for the contracting area and volume relations were found 1.08 and 1.04. Usually, for nucleation equations m takes values 2.00 and 3.00 [3, 19].

We have previously applied [5, 6, 17] a different method of studying this heterogeneous reaction by monitoring the change of the pH-value of the reaction mixture *vs*. time. We suggested that the dissolution process took place by the following reactions:

$$CH_3COOH \leftrightarrow CH_3COO^- + H^+ \qquad (7)$$

$$(CaCO_3)_S + H^+ \rightarrow Ca^{2+} + HCO_3^- \qquad (2a)$$

$$HCO_3^- + H^+ \leftrightarrow H_2CO_3 \qquad (8)$$

$$H_2CO_3 \rightarrow (CO_2)_{gas} + H_2O \qquad (9)$$

$$(CaCO_3)_S + H_2CO_3 \rightarrow Ca^{2+} + 2HCO_3^- \qquad (10)$$

We concluded that the transformation of H_2CO_3 to $CO_{2(gas)}$, i.e. reaction (9) is more likely to be the rate-controlling step in the range $2.37 \le pH \le 4.95$. In the pH-range from 3.96 to 6.40 mass transfer has a significant contribution to the determining step of the overall reaction.

The chemical processes, like dissolution processes, are accompanied by heat effects. Calorimetry represents a unique method to gather thermodynamics and kinetics results. The rate ($\dot{q}_{react}$) during a chemical reaction is proportional to the rate of conversion (r) and can be expressed in terms of the following mathematical expression [20, 21]:

$$\dot{q}_{react}(t) \sim r(t)V_r \qquad (11)$$

where V_r the reraction volume.

The task of the calorimeter is to determine the total heat flow rate ($\dot{q}_{tot}$) during a transformation. Generally, any kind of physical process in which heat is released or absorbed is measured. Therefore, the total can be expressed [21]:

$$\dot{q}_{tot} = \dot{q}_{react} + \dot{q}_{min} + \dot{q}_{phase} \qquad (12)$$

where $\dot{q}_{min}$ the heat flow rate occurring due to mixing and $\dot{q}_{phase}$ due to the phase changes.

The integration of the total (Q_{tot}) gives the heat balance equation:

$$Q_{tot} = \int_{t=0}^{t=t_f} \dot{q}_{tot}\,dt = \sum_{i=1\ldots N_R} (-\Delta_r H_i) n_i + Q_{mix} + Q_{phase} + Q_{error} \qquad (13)$$

where t_f is the integration limit in time, $\Delta_r H$ the reaction enthalpy, n_i the number of moles of the ith reaction component, Q_{mix} the heat of mixing, Q_{phase} the heat released or absorbed by phase change process,

and Q_{error} the sum of all measurement errors. For a twin vessel calorimeter, by using proper blanc process in the reference vessel, the Q_{mix}, Q_{phase} and Q_{error} are assumed to be negligible, meaning that:

$$Q_{tot} = Q_{react} = Q \text{ or } \dot{q}_{tot} = \dot{q}_{react} = \dot{q} \quad (14)$$

Once the reaction enthalpy is determined, it is possible to calculate the thermal conversion or fractional heat evolution of the reaction:

$$X_{thermal}(t) = \frac{\int_{\tau=0}^{\tau=t} \dot{q}_i \, dt}{Q} \quad (15)$$

This ratio of partial and total evolved heat can be used as a measure of reaction extent [20–23]. The rate of the reaction (r_A) can expressed then as follows:

$$r_A(t) = \frac{\dot{q}_i(t)}{V_r \Delta_r H} = -kC_{A,0}^n (1 - X_{thermal}(t))^n \quad (16)$$

where $C_{A,0}$ is the initial concentration of component A and n the reaction order.

In this work we studied the reaction mechanism of the selective dissolution of calcite from low-grade phosphate ores (Epirus area, Greece) by dilute acetic acid, based on an alternative dissolution methodology using a calorimeter.

Experimental

Materials

The chemical analysis of Greek phosphate ore was carried out using an EDXRF Spectro XEPOS apparatus (Spectro Analytical Instruments, GmbH Germany). The composition of phosphate ore was CaO 53.58±0.06, P_2O_5 11.91±0.01, SiO_2 1.54±0.01, SO_3 0.87±0.01, Na_2O 0.83±0.07, MgO 0.42±0.02, Al_2O_3 0.28±0.01, Fe_2O_3 0.20±0.01, SrO 0.15±0.01; the loss of ignition was estimated as 35.81%. Acetic acid solution (1 M) was prepared by dissolving glacial acetic acid (100 mass%- Ferak Laborat GmbH Berlin) with distilled water.

Methods

By crushing the material in a jaw crusher [3] we yielded sieved fractions of 500–250 μm of the natural phosphate ore (phosphorite). The dissolution process was carried out in a heat flow twin calorimeter (Type C.80.II, Setaram, France) using two identical membrane vessels, for the acid dissolution process, and for the reference. Phosphorite samples of 50 mg were put into the lower compartment of each vessel and closed by thin circular membrane of parafilm. A volume of 2 mL of acetic acid solution (1 M) and 2 mL of distilled water were added into the upper compartment of the sample and reference vessels, respectively. After complete stabilization of the baseline, the membranes of both sample and reference vessels were broken simultaneously by movable rods.

The enthalpy of the dissolution was determined from calorimetric experiments performed at 10.0, 14.3, 20.3, 24.6 and 28.0°C. The recorder calorimetric run were converted to ASCII files and transferred into Excel for numerical elaboration. At isothermal conditions, heat flux calorimeter output is heat flow rate *vs.* time ($\dot{q}$[mW]), and hence these data could be treated thermodynamically as well as kinetically. The rate is proportional to the rate of reaction, to the enthalpy change of the process, and to the amount of the reacting material. The total heat evolved during the course of a reaction (Q) is equal to the total number of moles of reacted material (A_0) multiplied by the change in molar enthalpy (ΔH) of the reaction. Similarly, the heat evolved at time t (q) is equal to the number of moles of reacted material (x), up to time t multiplied by the change in molar enthalpy for that reaction.

Hence, the conversion fraction (X_i) is equal to the heat evolved at time t divided by the total heat evolved during the course of a reaction.

The dissolution reaction has been also carried out in the batch mode. In a beaker placed into a thermostat bath, we added 3 g of phosphorite and 120 mL of acetic acid solution (1 M). After appropriate dissolution time, the remained solids were separated from supernatant solution by vacuum filtration, using membrane filters (Millipore, 0.22 μm). The concentration of phosphate ions in solution was determined by colorimetric method [24]. The solids were washed by distillated water and acetone.

FTIR was performed using a Bruker EQUINOX 55/S spectrophotometer. The KBr disk technique was employed and the infrared spectra were recorded in the region 4000–400 cm^{-1}, with resolution of 4.00 cm^{-1}.

The textural analysis of the particles before and after dissolution, were examined by scanning electron microscopy (SEM) using a Jeol JSM-6300 instrument.

Results and discussion

The calorimetric data are depicted in Fig. 1, and the results from the treatment of the corresponding curves are shown in Table 1. The curves of heat flow rate *vs.* time of the phosphorite dissolution for various temperatures show that the maximum rate ($\dot{q}_{max}$) was increased, whereas the time (t_{peak}) to achieve the corresponding $\dot{q}_{max}$ values was decreased, as the initial temperature was increased. The SETSOFT package has been used

Table 1 Analysis of rate curves

Temperature/°C	$\dot{q}_{max}$/mW	t_{max}/s	Q/J g^{-1}
10.0	3.9	465	–75.9
14.3	4.2	345	–81.4
20.3	5.0	265	–86.2
24.6	5.1	260	–95.4
28.0	5.6	240	–96.6

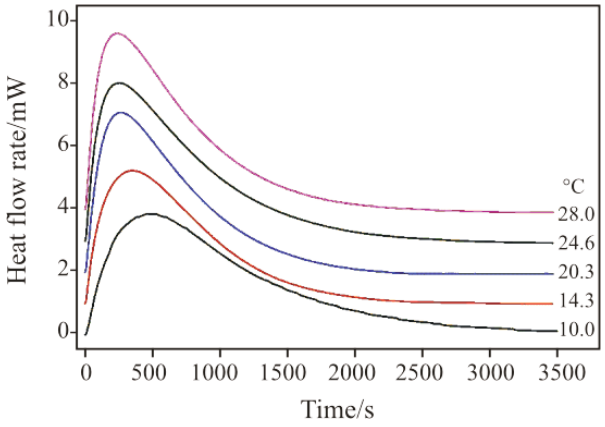

Fig. 1 Heat flow rate curves for the dissolution of phosphorite at various temperatures. The temperatures are indicated

for integration of the curves of heat flow rate *vs.* time, which provided the heat (Q, J g^{-1} of the initial mass of phosphorite) released during the complete of the dissolution process. The dissolution of the calcite species of phosphorite ore by dilute acetic acid is an exothermic effect. The absolute values of Q were increased from 75.9 to 96.6 kJ g^{-1}, as the experimental temperature was increased from 10.0 to 28.0°C.

The dissolution kinetic curves [X=$f(t)$] are illustrated in Fig. 2. The curve at temperature 10°C shows a sigmoid shape with end point at about 60 min. The curve at temperature 14.3°C shows more sharp initial

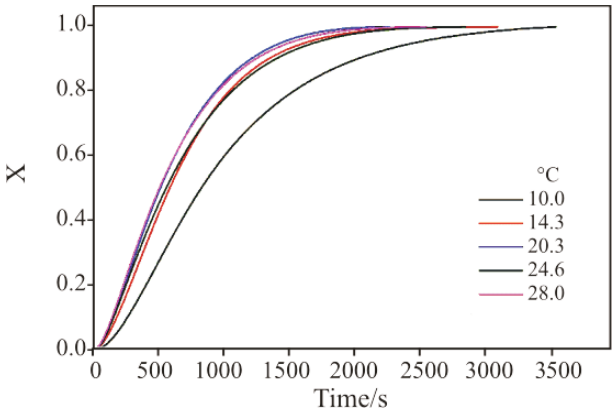

Fig. 2 Kinetics curves [X=$f(t)$] for dissolution of phosphorite at various temperatures

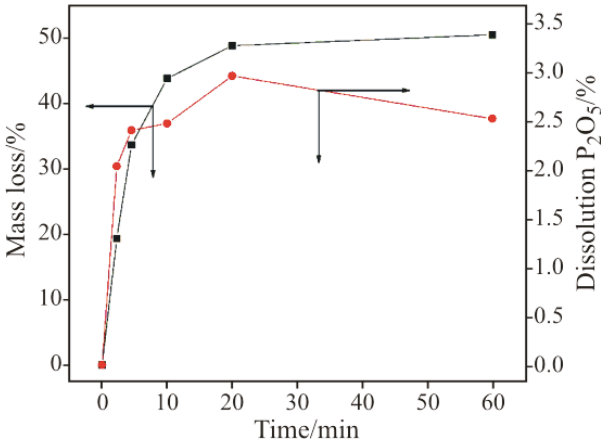

Fig. 3 The batch dissolution experiment. Mass loss and P_2O_5 dissolution *vs.* dissolution time

stage of dissolution, that is a larger dissolution rate, with end point about 50 min. The other three curves have shape similar to the curve at 14.3°C, but the end points are at about 42 min.

The results of the batch dissolution experiment are depicted in the Fig. 3. A rapid increase of the mass loss of solid phase up to 33.61% is observed at the first 4.5 min. In the same time the amount of dissolved phosphates was only 2.41% of the total P_2O_5. Taking into account the above results and the empirical formula of apatite we calculated that the 1.90% of mass loss was attributed to the apatite dissolution and the other 31.71% was attributed to the calcite dissolution mainly. The less rapid dissolution rate observed between dissolution time of 4.5 and 20 min. At dissolution time of 20 min the mass loss was 48.77% and the dissolved amount of phosphates was only 2.97%. The calculated amounts of dissolved apatite and calcite were 2.24 and 46.43%, respectively. At dissolution time of 60 min the mass loss was increased slightly up to 50.44%, while the dissolved phosphates were decreased to 2.53%. The slight decrease of the P_2O_5 in the supernatant solution is attributed to the adsorption of phosphate anions onto solid surface.

Figure 4 shows the infrared (IR) absorption spectra of solid samples un-treated and treated by acetic acid solution. The spectra of the un-treated solids (Fig. 4 dissolution time=0.00) show absorption bands of the corresponding absorption range of apatite and calcite. The broad band at 3100–3500 cm^{-1} corresponds to adsorbed water. Two sharp and weak peaks at 2517 and 1796 cm^{-1}, a broad peak at about 1435 cm^{-1} and two sharp peaks at 874 and 713 cm^{-1} are attributed to calcite adsorptions. As the dissolution time increases, the peaks at 2517, 1796 and 713 cm^{-1} gradually disappear, the sharp peak at 874 cm^{-1} decreases and shifts to 866 cm^{-1}, while the broad band at about 1435 cm^{-1} decreases and splits in two peaks at 1457 and 1428 cm^{-1}. The peaks at

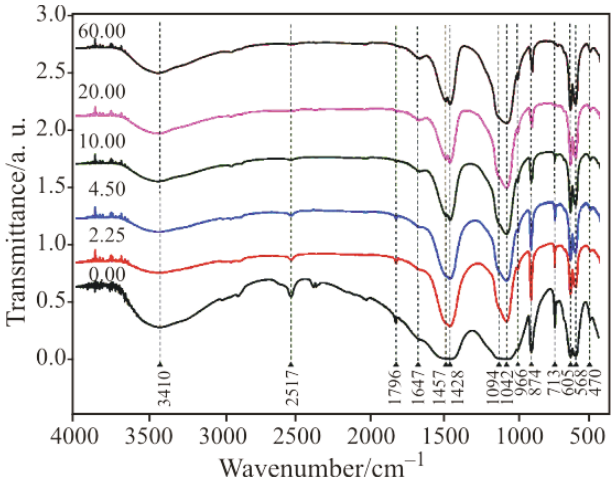

Fig. 4 FTIR spectra of remained solids after dissolution process. The dissolution time is indicated

866, 1457 and 1428 cm^{-1}, as well as at 1647, 1094, 1042, 966, 605, 568 and 470 cm^{-1} are attributed to francolite adsorptions.

The IR results are in accordance with the results of previous paragraph (mass loss and phosphate chemical analysis) and indicate that the dissolution process of phosphorite by acetic acid solution takes place mainly by calcite dissolution species.

In all cases, the pH values of the initial acetic acid solution, as well as these of the final one, were measured after the finish of dissolution process and mean values of 2.37 and 3.90, respectively, were found. According to our previous paper [5], in that pH region and at 25°C the transformation of H_2CO_3 to $CO_{2(gas)}$ (reaction (8)) is the rate-controlling step of the overall reaction. Demir *et al.* [25] found that for the leaching of magnesite ore by citric acid solutions the process was controlled by a chemical reaction.

The fitting of reaction model $\ln(1/(1-X))=kt^m$, for pseudo-homogeneous first order reaction model for several temperatures is depicted in Fig. 5, where it is clearly shown that the dissolution process took place in two steps. The duration of the first step is about 90 s (ln90=~4.5), whereas the second one occurs in the time range from 90 to about 1800 s (ln1800=~7.5). The kinetic results for the second step are summarized in Table 2. In all cases, Eq. (4) fitted perfectly the experimental data (R^2 ranged between 0.9959 and 0.9993 with a mean value of 0.9984); the parameter m varied in the range 1.37 to 1.55 with a mean value of 1.46. These values of m lie outside of the empirically established range for diffusion-limited mechanism (m=0.53–0.58) and they could rather be considered as approaching the ranges for area or volume contracting (m=1.04 and 1.08) and/or nucleation (m=2.00–3.00) mechanisms [3, 18]. The estimated values of rate constant (k) varied in the range

Table 2 Results from the fitting of reaction model $\ln(1/(1-X))=kt^m$

Temperature/°C	M	$k\cdot10^5$/s^{-1}	R^2
10.0	1.55	1.9	0.9959
14.3	1.51	4.5	0.9989
20.3	1.48	6.7	0.9991
24.6	1.37	11.5	0.9989
28.0	1.40	11.3	0.9993
Mean	1.46	7.2	0.9984

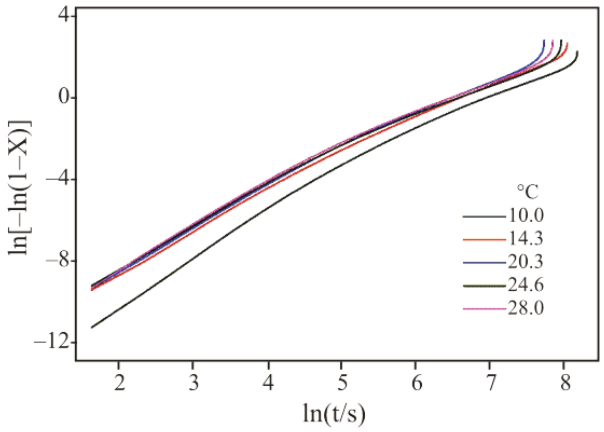

Fig. 5 Analysis of reaction model $\ln(1/(1-X))=kt^m$ of the rate law for the heat evolved at time t (q)

$1.9\cdot10^{-5}$ to $11.5\cdot10^{-5}$ s^{-1}. However, in a previous paper [3] we estimated much smaller values of m, whereas the values of k were found much larger, depending on the liquid/solid ratio, i.e. on the acid-carbonate stoichiometry, by using two sets of experiments with stoichiometry of 0.78 and 1.25. In that case, the values of m were estimated as 0.358 and 0.447, respectively, whereas the corresponding values of k were estimated as 0.0973 and 0.0736 s^{-1}, respectively. In the present paper, the stoichiometry was set at about 3.78,

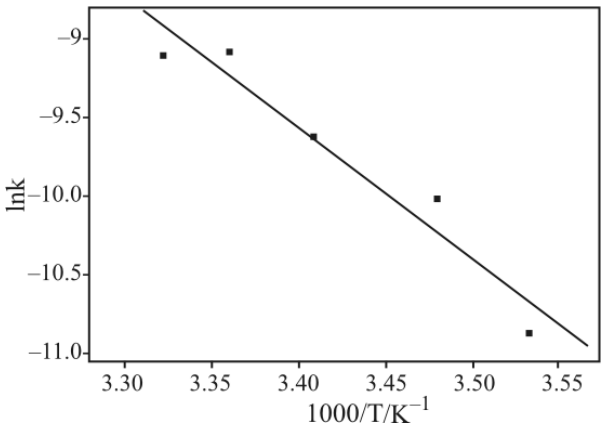

Fig. 6 Arrhenius plot determining the apparent activation energy (E_α), from the estimated values of the rate constant (k)

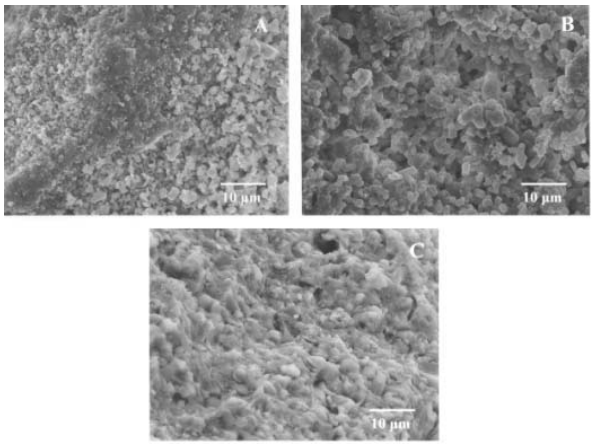

Fig. 7 SEM photographs of the a – raw phosphorite and b, c – after dissolution

and we assume that increasing the stoichiometry resulted in increased m values, whereas the values of the rate constant (k) are decreased.

An Arrhenius-like equation was found which relates temperature and estimated rate constant k of the dissolution reaction model $\ln(1/(1-X))=kt^m$ (Fig. 6), of which the E_α was determined as 69.7 kJ mol^{-1}. A similar value of activation energy was found for the leaching of calcareous phosphate rock by succinic acid (64.92 kJ mol^{-1}) [8], for the leaching of magnesite by citric acid solutions (61.35 kJ mol^{-1}) [25], as well as for dissolution of calcite in concentrated aqueous sodium dichromate solution (55–84 kJ mol^{-1}) [26].

In Fig. 7 are depicted SEM micrographs of raw phosphorite (a) and acid dissolution samples (b and c). On the surface of the raw sample we observed small particles sized from ~0.5 to ~5 μm. However, the particles of the phosphorite showed two different textures after acid dissolution; some of them are constituted from relatively big particles with size between 2 and 10 μm, whereas large halls have been also formatted (Fig. 7b). Other particles appeared with an apatitic crust surface showing botryoidally and mammillary forms (Fig. 7c). These two different kinds of particles may explain the two steps of the hemi-empirical reaction model $\ln(1/(1-X))=kt^m$.

Conclusions

The calorimetric data have been used successfully for thermodynamic and kinetic studies of the phosphorite dissolution by dilute acetic acid. The dissolution enthalpy of (Q) were increased from 13.1 to 16.7 kJ mol^{-1}, as the experimental temperature was increased from 10.0 to 28.0°C.

The batch dissolution experiment point at the main process was the calcite than apatite dissolution.

The reaction model with general form, $\ln(1/(1-X))=kt^m$, was found to fitted the experimental data regardless of the experimental temperature. The estimated values of m and k of the reaction model seem to depend on the acid-carbonate stoichiometry.

These reaction model fitting and the SEM microphotographs were assigned in the presence of two different kinds of particles in the phosphorite.

The activation energy (E_α) of the dissolution process was estimated as 69.7 kJ mol^{-1} by using an Arrhenius relation connecting the calculated dissolution rate constants (k) from the reaction model and the temperature.

Acknowledgements

The authors are grateful to the Ring of Laboratory Units and Centers of University of Ioannina for calorimetric measurements and SEM photographs. We also thank Dr Petrakis and SPECTRO Analytical Instruments for EDXRF analysis.

References

1 W. Sadeddin and S. I. Abu-Eishah, Int. J. Miner. Process, 30 (1990) 113.
2 S. I. Abu-Eishah, I. S. El-Jallad, M. Muthaker, M. Tougan and W. Sadeddin, Int. J. Miner. Process, 31 (1991) 115.
3 E. D. Economou and T. C. Vaimakis, Ind. Eng. Chem. Res., 36 (1997) 1491.
4 T. C. Vaimakis and E. D. Economou, Ind. Eng. Chem. Res., 37 (1998) 4306.
5 E. D. Economou, T. C. Vaimakis and E. M. Papamichael, J. Colloid Interface Sci., 201 (1998) 164.
6 E. D. Economou, T. C. Vaimakis and E. M. Papamichael, J. Colloid Interface Sci., 245 (2002) 133.
7 E. M. Papamichael, E. D. Economou and T. C. Vaimakis, J. Colloid Interface Sci., 251 (2002) 143.
8 M. Ashraf, Z. I. Zafar and T. M. Ansari, Hydrometallurgy, 80 (2005) 286.
9 L. N. Plummer, D. L. Parkhurst and T. M. L Wigley, Chemical Modeling in Aqueous System, E. A. Jenne, Ed. Amer. Chem. Symp. Ser., 93 (1979) 537.
10 L. N. Plummer, T. M. L Wigley and D. L. Parkhurst, Amer. J. Sci., 278 (1978) 179.
11 R. G. Compton and G. H. W. Sanders, J. Colloid Interface Sci., 158 (1993) 439.
12 C. A. Brown, R. G. Compton and C. A. Narramore, J. Colloid Interface Sci., 160 (1993) 372.
13 E. L. Sjöberg and D. T. Rickard, Geochim. Cosmochim. Acta, 48 (1984) 485.
14 M. H. Al-Khaldi, H. A. Nasr-El-Din, S Mehta and A. D. Al-Aamri, Chem. Eng. Sci., 62 (2007) 5880.
15 E. D. Economou, N. P. Evmiridis and A. G. Vlessidis, Ind. Eng. Chem. Res., 35 (1996) 465.

16 J. W. Morse and R. S. Arvidson, Earth-Sci. Rev., 58 (2002) 51.
17 T. C. Vaimakis and E. M. Papamichael, Encyclopaedia of Surface & Colloid Science, A. Hubbard, Ed., Marcel Dekker, Inc., New York 2002, pp. 1471–1485.
18 S. F. Hulbert and D. E. Huff, Clay Miner., 8 (1970) 337.
19 C. H. Bamford and C. F. H. Tipper, Comprehensive Chemical Kinetics, Vol. 22, Reactions in the Solid State, Elsevier Scientific Publishing Co., Amsterdam, The Netherlands 1980, p. 78.
20 O. Levenspiel, Chemical Reaction Engineering. 2nd Ed.; John Wiley and Sons, New York 1972.
21 A. Zogg, F. Stoessel, U. Fischer and K. Hungerbühler, Thermochim. Acta, 419 (2004) 1.
22 C. LeBlond, J. Wang, R. D. Larsen, C. J. Orella, A. L. Forman, R. N. Landau, J. Laquidara, J. R. Sowa, D. G. Blackmond and Q. K. Sun, Thermochim. Acta, 289 (1996) 189.
23 F. Stoessel, J. Thermal Anal., 49 (1997) 1677.
24 P. G. Jefery, Chemical Methods in Rock Analysis, 2nd Ed, Pergamon Press, New York 1975.
25 F. Demir, B. Donmez and S. Colak, J. Chem. Eng. Jpn., 36 (2003) 683.
26 T. Wang and Z. Li, J. Colloid Interface Sci., 281 (2005) 130.

Received: March 5, 2007
Accepted: October 30, 2007

DOI: 10.1007/s10973-007-8025-8